Structural and electronic properties of PANI-ZnO-TiO_2 nanocomposite

N. A. Niaz, [a*], A. Shakoor[a], F. Hussain[a], M. Iqbal, N.R. Khalid[c], M. K. Saleem[a], N. Anwar[a], J. Ahmad[a],
[a]*Polymer Research Lab, Institute of Physics, Bahauddin Zakariya University, 60800, Multan, Pakistan*
[b]*Department of Battery Research and Development, Daimler Truck Asia, Mitsubishi Fuso Truck and Bus corporation (MFTBC) 2118522, JAPAN*
[c]*Department of Physics, University of OKARA*

The nanocomposites of doped Polyaniline (PANI) with ZnO-TiO_2 nanoparticles have been prepared by in-situ polymerization method. The structural properties of synthesized PANI and PANI/ZnO-TiO_2 were studied by X-ray diffraction (XRD) analysis. XRD pattern show that PANI is intercalated into the layers of ZnO-TiO_2 successfully and thus the degree of crystallinity increases due to crystalline nature of ZnO-TiO_2. FTIR analysis indicated that there is a strong interaction between ZnO-TiO_2 nanoparticles and PANI. Electronic properties (Dielectric and Conductivity) of PANI and PANI/ZnO-TiO_2 nanocomposite have been investigated between frequency ranges from 20Hz to 01MHz, higher dielectric constants and dielectric losses of PANI/ZnO-TiO_2 nanocomposites were found. As the content of ZnO-TiO_2 increased, the dielectric constant and loss also increased. The value of dielectric constant for all samples is very high at low frequency but decreases with increase in frequency. Synthesis of PANI/ZnO-TiO_2 nanocomposite materials with a large dielectric constant is promising for charge storage devices applications.

(Received July 7, 2022; Accepted October 27 2022)

Keywords: Nanocomposite, Dielectric, Conductivity, Polymer, Morphology

1. Introduction

Conducting polymer/inorganic composites, which possess unique physical and chemical properties, have attracted more and more attention. Due to their outstanding properties, conductive polymers with a polyaromatic backbone, including polypyrrole (PPy) and polyaniline (PANI), have established a great deal of care in the last three decades [1–5]. Typically, prodigious efforts have been made to improve their mechanical, chemical, and thermal stability, optical properties, conductivity and electro-activity, and so on. In this situation, more focus is to fabricate and study of nanocomposites that contain these sort of polymers. The polymers are predictable to help from the attractive properties of the supplementary materials. To attain such a collaboration, the control of nanoparticle interfaces, the structural and chemical properties of the polymer chains must be significant [6-7]. Among various combinations, nanocomposites made of metal oxides and conductive polymers have achieved excellent properties. Preceding studies have revealed that the incorporation of metal oxides can efficiently improve the electrical, mechanical, and dielectric properties of various conductive polymers [8–10]. Predominantly, much research has been attentive on PANI, which shows good electrical conductivity, anion or cation exchange behavior, ambient stabilityand simple polymerization over different metal oxides [11–17].

Several different metals and metal oxide nanoparticles have so far been encapsulated into the shell of conducting polymers, giving rise to a host of composites [18–24]. These composite materials have shown better mechanical, physical, and chemical properties. However, TiO_2 is considered as n-type semiconductor due to the existence of oxygen gaps in TiO_2 lattice. These gaps are created with the emission of two electrons and molecular oxygen leaving oxide ion vacancy states [25]. Titanium dioxide was utilized widely as photo-catalyst due to its vital and

* Corresponding author: niazpk80@gmail.com
https://doi.org/10.15251/JOR.2022.185.713

extraordinary properties. TiO_2 has direct band gap 3.0 to 3.2 eV. TiO_2 [26-28]. While ZnO is direct band gap semi-conductor of the group II-VI semiconductor group possessing energy gap 3.37eV helpful for electronic devices applications [29-32]. Electronic properties (Dielectric and Conductivity) of conducting polymer polyaniline containing a nano semiconducting material have not so far studied in detail. In this work, an approach is reported to synthesize the PANI-ZnO-TiO_2 nanocomposites by In-situ polymerization. The structural properties and morphology of prepared nanocomposite were investigated by X-ray diffraction (XRD), Fourier-transform infrared (FTIR) spectroscopy and scanning electron microscopy (SEM). Excellent electronic properties (Dielectric and Conductivity) of PANI-ZnO-TiO_2 nanocomposites reveals that synthesis compound is useful for charge storage applications.

2. Experimental Details

2.1. Chemicals and materials

The Aniline was purched from Fluka. Ammonium persulphate (APS), Titanium dioxide (TiO_2) and Zinc oxide (ZnO) were obtained from Sigma Aldrich. 37% w/w concentrated HCl and distilled water were also used for the preparation of required compounds.

2.2. Synthesis of Polyaniline (PANI)

The required amount of APS was dispersed in 200 mL of distilled water and stirred for 5h, after that aniline was dispersed gradually in the suspension during stirring at 5°C. 37% w/w concentrated HCl was added dropwise maintain pH up to 1.The molar ratio of monomer to oxidant was kept 1:1. The suspension was left 24 hrs for polymerization. After all, the suspension was filtered and washed with distilled water. The greenish black paste of PANI was acquired which was dried at 60°C in vacuum oven for 24 hrs.

2.3. Synthesis of PANI-ZnO-TiO_2 nanocomposites

The ZnO-TiO_2 powder (1:1) was mixed in 200 mL distilled water under strong magnetic stirring to prepare the PANI-ZnO-TiO_2 nanocomposite. 10 ml aniline was added dope wise and the solution was left stirring for 6 h. 37% w/w concentrated HCl was also added in to aniline solution to maintain pH up to 1. Calculated amount of ammonium per-sulphate (APS) was added drop wise, while molar ratio of oxidant to monomer was kept 1: 1. The mixture was turned to greenish black color, indicating that the organic polymerization reaction has started. The solution was left for 24hrs, and filtered. A dark black-green paste of PANI-ZnO-TiO_2 nanocomposites was obtained which was washed with distilled water. The paste was dried at 60°C in a vacuum oven for 24 hrs.

2.4. Measurements

Electronic properties (Dielectric and Conductivity) were measured by using a two-point method in the frequency range 20 Hz to 1MHz. The samples were connected to a Keithley 2400 electrometers and a current source electrometer. The dielectric constant of all the samples and reproducibility were checked. X-rays powder diffraction analysis was carried out using an automated diffractometer, Panalytical X' Pert PRO equipped with CuKα radiations (λ = 1.54 Å). The instrument was operated at 40 kV and 30 mA and diffraction patterns of PANI and PANI-ZnO-TiO_2 nanocomposites samples mounted on a standard holder were recorded over the range of 10 to 70° at scane rate 2°/min. The FTIR spectra were recorded on KBr pellet samples in the range of 4000-500 cm^{-1} by using a Perkin Elmer Fourier transform infrared spectrometer. Scanning Electron Microscopy (SEM) was carried out on EVO50 ZEISS instrument.

3. Results and discussion

3.1. Structural Analysis

The XRD patterns of various weight ratio of TiO_2-ZnO (1:1) [33-34] composite with different ratio of PANI have been shown in Fig 1.The XRD results reveals that hkl values (120),

(110) , (012), (220), (111), (210), (231), (320), (241), (160), (203), (201), (332) and (301) confirm the anatae phase of TiO_2 and zincate phase of zinc oxide which can be confirmed by comparing with.

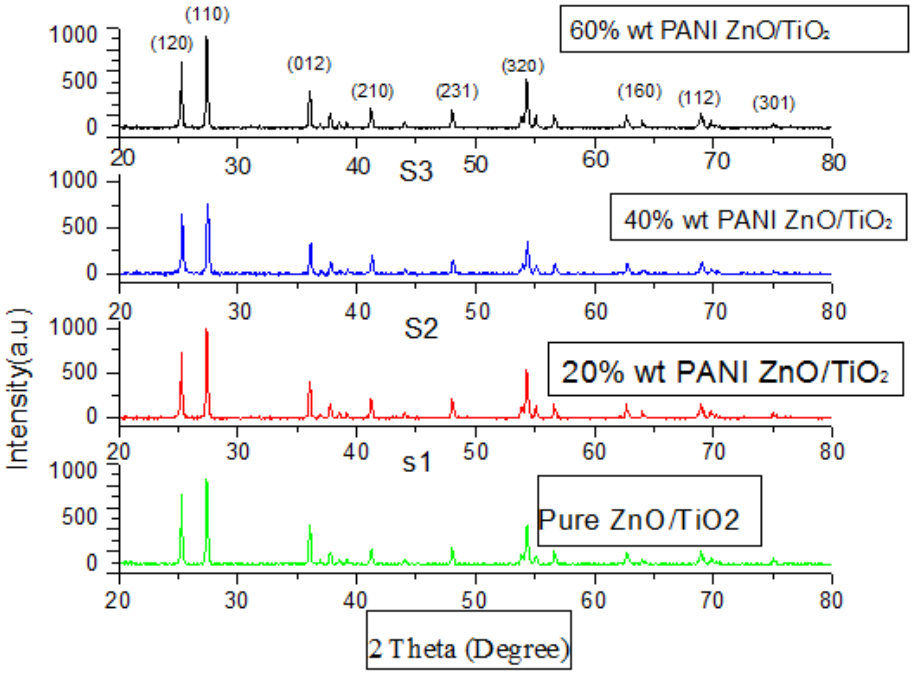

Fig. 1. Shows XRD patterns of pure and ZnO/TiO2 polyaniline nanocomposites. The JCPDS card number (00-021-1272) and (00-036-1451).

The pattern of nanocomposites of ZnO/TiO_2 with different ratio of polyaniline show the crystalline in nature. The hexagonal phase of Zinc oxide and tetragonal phase of TiO_2 was also confirmed by XRD patterns. By using Scherer's formula, the crystallites size of PANI-ZnO-TiO_2 nanocomposite was estimated as 70-90 nm [35-36]. There are some additional peaks observed at 2θ values of 27.43 and 44.25 may be attributed to presence of polyaniline. Also, it has been noticed that there is an increase in the intensity which suggests that crystallinity has been improved with the addition of ZnO/TiO_2 into PANI.

3.2. FTIR Analysis

FT-IR spectra shown in Fig.2 elucidate functional groups of PANI as well as to confirm the presence of polyaniline in the TiO_2/PANI composite to act as catalyst. Various vibrational peaks observed in these spectra are listed in the following Table1 along with their possible assignments. It is already known that FTIR spectrum of PANI consists of main peaks at 1595, 1490, 1308, 1295, and 1046 cm^{-1} [37]. However, some of the vibrational peaks observed in the present TiO_2/PANI composites match with these above-mentioned vibrations, while some other vibrational peaks show slight shifting either towards higher or lower wave numbers depending on the composition and nature of the nanocomposite materials. Along with these vibrations, some other vibrations are also observed in the low wave number range between 900 and 450 cm^{-1} as obvious from Fig.2. These vibrations can be attributed to metallic bonding. The composite catalysts show vibrational peaks at or around 503 cm^{-1} (496.04, 491.18, 479.15 cm^{-1}) (see Fig. 2), which might correspond to Ti-O bond and it is due to presence of TiO_2 in the composite [38]. Shifting of the observed vibrational bands related to Ti-O bonds as compared to the FTIR spectrum of TiO_2 nanoparticles appears to be caused by interactions between TiO_2 and PANI structures. The observed vibrational band around 479 cm^{-1} might also be pointed out to be due to Zn-O stretching frequency [39-40]. In addition, it is also noted that benzene rings in polyaniline

structure are also present and are associated with a significant C-H out of plane bending peak around 1475 cm^{-1}. The absorption peaks around 1490 cm^{-1} and 1595 cm^{-1} wave numbers may be related to the C-C stretching mode of benzoid and quinoid rings of PANI molecules respectively [41].

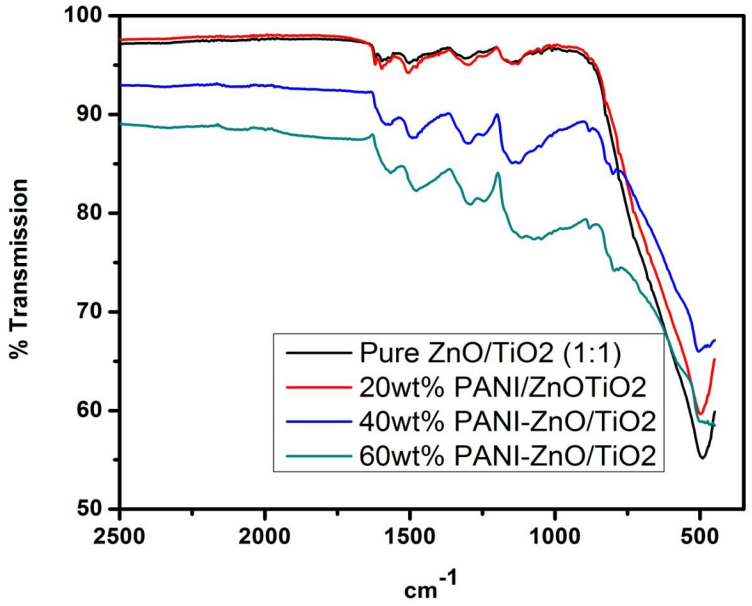

Fig. 2. Shows FTIR spectra of TiO_2/ZnO polyaniline nanocomposites.

Shifting of bands might be associated with the action of hydrogen bonding between the hydroxyl groups on the surface of ZnO/TiO_2 nanoparticles and the amine groups in the PANI molecular chains. Such interaction between PANI and ZnO/TiO_2 nanoparticles has also been confirming the formation of polyaniline in these nanocomposites.

Table 1. FTIR characteristic peaks and their assignments.

Sr. No.	ZnO/TiO_2 (1:1)	20wt% PANI-ZnO/TiO_2	40wt% PANI-ZnO/TiO_2	60wt% PANI-ZnO/TiO_2	Peak assignments
1	491.18	496.04	503.09	479.15	508 (Ti—O) 448-550 (Zn—O stretching vibration)
2			799.40	794.19	800 out of plane C—H vibration
3			880.37	879.21	900 out of plane C—H vibration
4		1009.99		1046.44	1030 (Stretching vibration of N=Q=N rings)
5	1148.56	1146.87	1145.86	1111.78	1100 (C—N Bond)
6	1308.98	1295.76	1298.35	1244.03 1289.32	1297.38 (C—H Bending)
7	1502.26	1502.71	1490.96	1475.33	1479,1496 (C=C Stretching mode of benzoid ring)
8	1595.49	1595.62	1566.99	1565.54	1561,1592 (C=C Stretching mode of Quinoid rings)
9	1618.40	1618.39			(C=C Stretching mode of Quinoid&Benzoid ring)

3.3. Scanning electron microscopy (SEM)

The Surface morphology of the PANI-ZnO-TiO_2 nanocomposites samples was evaluated using SEM micrographs. Fig.3 (a-d) displays SEM micrographs of TiO_2/ZnO polyaniline which clearly indicate that the crystallites are nearly spherical, somewhat elongated, and randomly oriented and distributed throughout the micrograph. Moreover, some crystallites depict agglomeration of small particles. The SEM micrographs of the prepared TiO_2/ZnO/PANI composites with ZnO/TiO_2 to PANI ratio of 20% to 60% as displayed in Fig.3 (a-d) reveal the formation of a thin layer of polyaniline molecules on the TiO_2/ZnO particles. These SEM micrographs of TiO_2/ZnO composites with different ration of PANI demonstrate the synthesis of a uniformly dispersed additive coating on these nanocomposites.

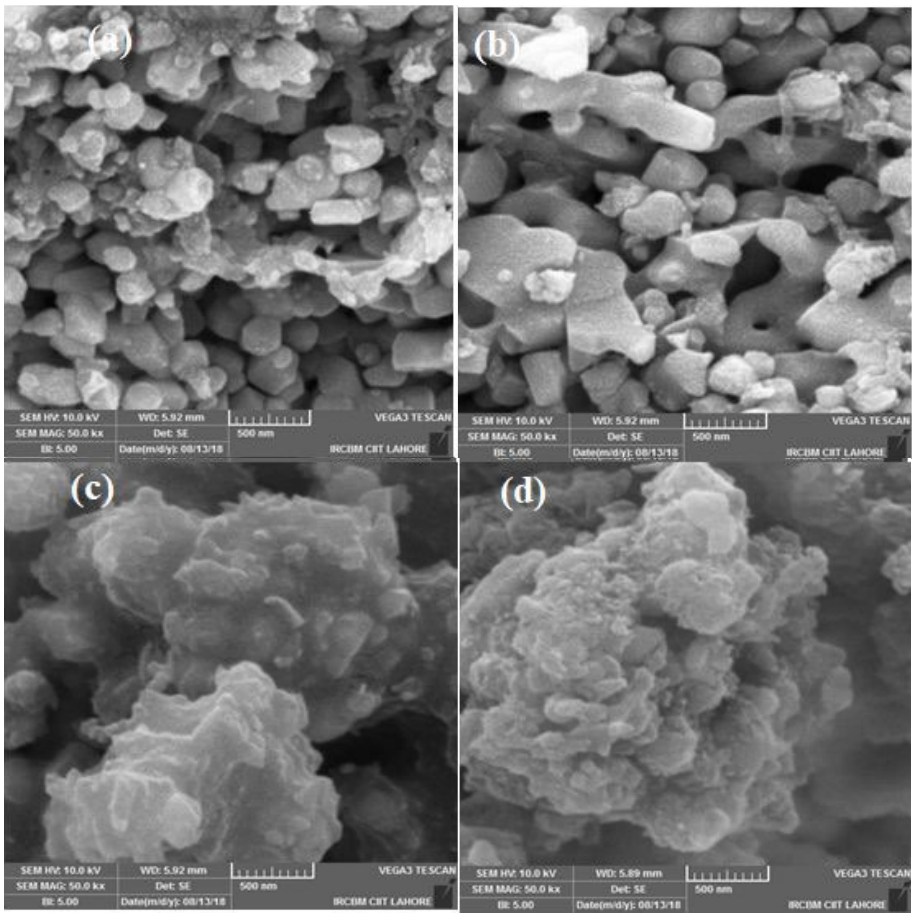

Fig. 3. Shows SEM image of PANI-ZnO-TiO_2 nanocomposites (a) TiO_2/ZnO (1:1). (b) 20% wt % PANI-TiO_2/ZnO (c) 40% wt%PANI-TiO_2/ZnO (d) 60 wt % PANI-TiO_2/ZnO.

3.4. Dielectric Properties

3.4.1. Dielectric constant

The dielectric properties have been investigated under the influence of the applied field at room temperature in the frequency range of 20Hz to 1MHz.

The dielectric constant, ε_r is calculated by the given formula

$$\varepsilon_r = \frac{cd}{A\varepsilon_\circ} \tag{1}$$

where c and d represent the capacitance and sample thickness and $\varepsilon_\circ$ is the permittivity of free space. It is supposed that the polyaniline plays the role of an amphoteric dopant in the polyaniline-doped ZnO/TiO_2 nanocomposite. The polyaniline ions have ability to approach both lattice and

interstitial sites. So polyaniline is expected to take the place of Zn ions in the lattice located at the grain boundary in priority and might play role of acceptor and approaches to the deep level trap. It has been shown in the Fig.4, that the dielectric constant decreases rapidly with the applied ac field. This decrease is due to the increment in the ion jumping from one level to the other and due to the enhanced space charge which is shown by the samples. The maximum number of atoms occupies the grain boundaries that become active and play the role of charge catching. The large increase in the dielectric constant at lower frequencies is due to the enhanced space charge polarization caused by the rotation at the interfaces. It is said that the dielectric constant of the material should be larger than as compared to those traditional samples. This is due to the enhanced space charge polarization because of the morphology of their grain limit interface. Sharp increase of the dielectric constant rules out the dielectric loss at lower frequencies and temperatures. At smaller frequencies; there is clarity in the strength of the frequency dependence. There is a reduction in the dielectric constant with the rising value of the frequency; this is attributed to the inhomogeneity in the dielectric constant [32].

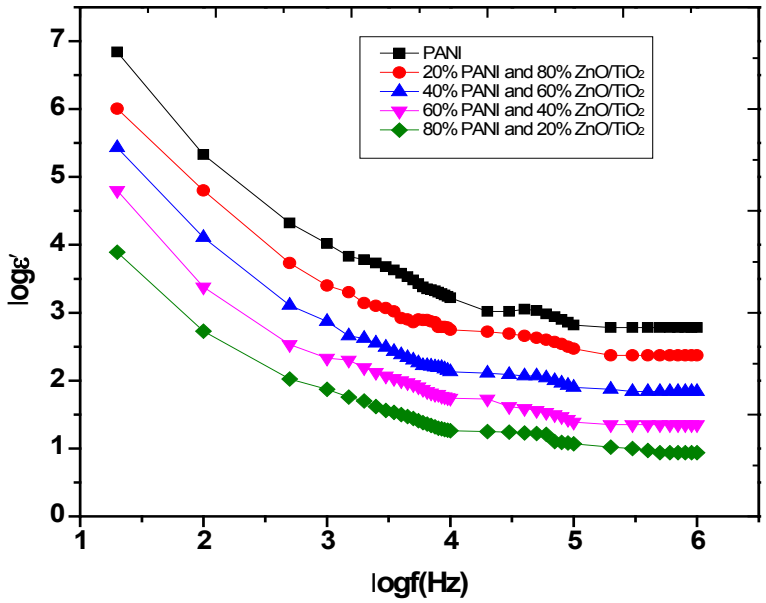

Fig. 4. Shows variations of dielectric constant versus log of applied frequency.

3.5. Dielectric loss

Figure 5 below clearly shows the changes in the dielectric loss with the variation in the applied frequency. It has been seen that the dielectric loss reduces with the increase in the applied frequency. The decrease in the angle at larger frequency is nearly same for all samples. There is some required energy for the orientation of the polar molecules in the direction of the applied field and this leads to the overall loss in energy. The in homogeneities relevant to the defects and space charge sequence in the inter phase generates absorption currents resulting in the dielectric loss. So when the frequency is increased then loss is observed due to the space charge polarization. It is also known that the reduction in loss occurs as the frequency increases and it gets reduced at higher frequency region [33].

Dielectric loss reduces with increasing frequency because of space charge polarization, measured by the formula

$$D = \tan\delta = \ddot{\varepsilon}/\acute{\varepsilon}. \quad (2)$$

The value of D decreases as the applied f increases, at lower f the higher value of D is due to orientation of molecules in the direction of applied field because their orientation occurs by

overcoming the frictional forces. Energy is loss or at high f the smaller value of D is because of reduced frictional forces because molecules have been oriented in the direction of field.

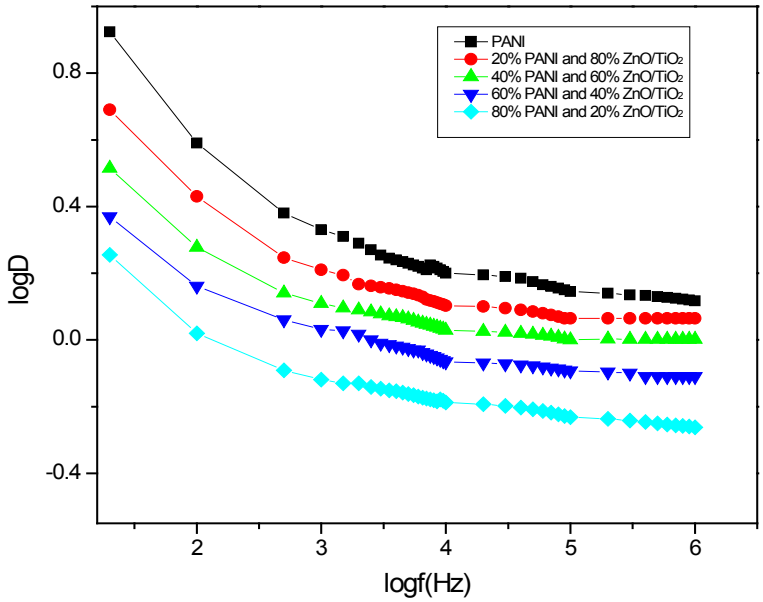

Fig. 5. Shows variations of dielectric loss versus applied frequency.

3.6. AC conductivity

An investigation has been made to measure the AC conductivity from the pellets made of polyaniline doped ZnO/TiO_2 nanocomposite.The AC conductivity can be found by the following formula:

$$\sigma_{AC} = 2\pi\varepsilon_0\varepsilon_r f \tan\delta \quad (3)$$

In this equation $\varepsilon_0$denotes the permittivity of the free space, f is the frequency, ε_r is the dielectric constant and tan δ is the loss factor. The below figure 6 shows the variation of AC conductivity versus the applied frequency.

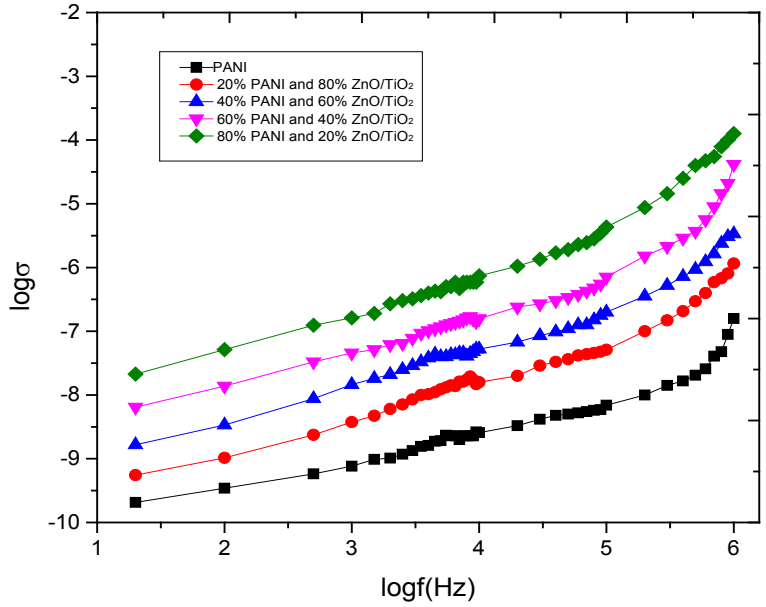

Fig. 6. Shows variation of AC conductivity versus applied frequency.

There has been noted an increase in the conductivity with increase in the frequency. Such a rise may be due to small-range hopping of the charge carriers between localized states. This rapid increase in the conductivity is due to larger polaron jumping. There is an increase in the AC conductivity with the increase in the frequency of the applied field. This is due to that when frequency has been increased then there is larger chance of hopping of electron [34].

4. Conclusion

Composites of Polyaniline (PANI) with ZnO-TiO_2 nanoparticles have been prepared by in-situ polymerization method. The crystallinity of synthesized samples was studied by XRD diffraction pattern and was found to be improved due to crystalline nature of ZnO-TiO_2 in PANI-ZnO-TiO_2sample.FTIR analysis indicated that there is a strong interaction between ZnO-TiO_2 nanoparticles and Polyaniline. Dielectric characterization demonstrated thatZnO-TiO_2 nanoparticles show a strong effect on the dielectric properties of resultant PANI-ZnO-TiO_2nanocomposites. The increased dielectric constant is recognized to the creation of an improved charge transport network in the comparatively insulating PANI. Synthesis of materials with a large dielectric constant is very essential for the improvement of charge storage devices.

References

[1] Gangopadhyay,R. De, A., Conducting polymer nanocomposites: a brief overview, Chem. Mater., 2000;12: 608-622; https://doi.org/10.1021/cm990537f

[2] Li, X.W., Wang, G.C., Li,X.X., Surface modification of nano-SiO2 particles using polyaniline, Surf. Coat. Tech., 2005;197: 56-60; https://doi.org/10.1016/j.surfcoat.2004.11.021

[3] Cardin D. J., Encapsulated conducting polymers, Adv. Mater. 14 (2002), 553-563; https://doi.org/10.1002/1521-4095(20020418)14:8<553::AID-ADMA553>3.0.CO;2-F

[4] Zhang L.J. and Wang M.X., Polyaniline/TiO2 Composite Nanotubes, J. Phys. Chem. B, 2003;107:6748-6753; https://doi.org/10.1021/jp034130g

[5] Skunik, M., Chojak, M., Rutkowska,I. A. Kulesza P. J., Improved capacitance characteristics during electrochemical charging of carbon nanotubes modified with polyoxometallate monolayers, Electroch. Acta., 2008; 53: 3862-3869; https://doi.org/10.1016/j.electacta.2007.11.049

[6] J.X. Huang, J. A. Moore, J. H. Acquaye and Kaner R. B., Mechanochemical route to the conducting polymer polyaniline, Macromolecule. 2005; 38: 317-321; https://doi.org/10.1021/ma049711y

[7] Guo, H.F., Zhu,H., Lin H.Y.Zhang J.Q., Polyaniline/Fe3O4 nanocomposites synthesized under the direction of cationic surfactant, Mater. Lett. (2008);62: 2196-2199; https://doi.org/10.1016/j.matlet.2007.11.047

[8] Sertchook H. Avnir D., Submicron silica/polystyrene composite particles prepared by a one-step sol− gel process, Chem.Mater., 2003; 15: 1690-1694; https://doi.org/10.1021/cm020980h

[9] Cui G., Lee J. S., Kim S. J., Nam, H., Cha,G. S.Kim, H. D., Potentiometric pCO 2 sensor using polyaniline-coated pH-sensitive electrodes, Analyst, 1998; 123: 1855-1859; https://doi.org/10.1039/a802872i

[10] A.A. Karyakin, L.V. Lukachora, E.E. Karyakina, and G.P. Kappachora:, The improved potentiometric pH response of electrodes modified with processible polyaniline. Application to glucose biosensor, Analy. Commun. 1999; 36: 153-156; https://doi.org/10.1039/a900597h

[11] Ayad, M.M., Salahuddin, N., Sheneshin, M.A., Optimum reaction conditions for in situ polyaniline films ,Synth. Metal, 2003; 132: 185-190; https://doi.org/10.1016/S0379-6779(02)00446-0

[12] Parvatikar N., Jain S., Kanamadi C.M., Prasad, M.V.N.A., Electrical and humidity sensing properties of polyaniline/WO3 composites, SensorSens. Actu. B: Chem.2006; 114: 599-602;

https://doi.org/10.1016/j.snb.2005.06.057

[13] Nagaraja,M., Pattar J., Shashank N., Manjanna, J., Mahesh,H.M., Electrical, structural and magnetic properties of polyaniline/pTSA-TiO2 nanocomposites, Synth. Met. 2009;59:718-722; https://doi.org/10.1016/j.synthmet.2008.12.025

[14] Mtsuo,Y., Higashika,S., Kimura,K., Miyamoto,Y. Sugie Y., Synthesis of polyaniline-intercalated layered materials via exchange reaction, J0urnal of Material Chemistry, 12 (2002), 1592-1596; https://doi.org/10.1039/b107436a

[15] Jiang J., Ai L.H., Qin D.B., Liu H.,Li, L.C., Preparation and characterization of electromagnetic functionalized polyaniline/BaFe12O19 composites, Synth. Met. 2009;159: 695-699; https://doi.org/10.1016/j.synthmet.2008.12.021

[16] Schnitzler,D.C., Meruvia, M.S., Hqmmelgen,I.A.,Zarbin,A.J.G. Preparation and Characterization of Novel Hybrid Materials Formed from (Ti,Sn)O2 Nanoparticles and PolyanilineChem. Mater.2003;15: 4658-4665; https://doi.org/10.1021/cm034292p

[17] Zeng, C.C., Han X.M., Lee, L.J., Koelling, K.W.Tomasko D.L., Polymer-clay nanocomposite foams prepared using carbon dioxide,Adv. Mater. 2003;151: 743-1747; https://doi.org/10.1002/adma.200305065

[18] Dhawan S.K., Singh K.,Bakhshi A. K., Ohlan. A.Conducting polymer embedded with nanoferrite and titanium dioxide nanoparticles for microwave absorption, Synth. Met. 2009;159: 2259-2262; https://doi.org/10.1016/j.synthmet.2009.08.031

[19] Huisman, C. O., Reller, C. L., Photoinduced reactivity of titanium dioxide, Prog. Sold. State Chem. 2004; 32: 32-33; https://doi.org/10.1016/j.progsolidstchem.2004.08.001

[20] Y. F. Shen, T. Xiong, T. Li, K. Yang, Tungsten and nitrogen co-doped TiO2 nano-powders with strong visible light response, Appl. Cataly. B: Envir.2008; 83: 177-185; https://doi.org/10.1016/j.apcatb.2008.01.037

[21] Yang X., Cao, C., Erickson, L., Hohn,K., Maghirang, R.., Klabunde, K.,Photo-catalytic degradation of Rhodamine B on C-, S-, N-, and Fe-doped TiO2 under visible-light irradiation, Appl.Cat.. B: Environ. 2009; 91: 657-662; https://doi.org/10.1016/j.apcatb.2009.07.006

[22] Zhou M., Yu, J., Cheng, B., Yu,H., Preparation and photocatalytic activity of Fe-doped mesoporous titanium dioxide nanocrystalline photocatalysts, Mater. Chem. Phys.2005;93: 159-163; https://doi.org/10.1016/j.matchemphys.2005.03.007

[23] Norton, D.P., Ivill, M., Li, Y., Kwon, Y.W., Erie, J.M., Kim, H.S., Ip, Y.W., Kim, S. and Kang, B.S.,Charge carrier and spin doping in ZnO thin films. Thin Sol. Fil. 2006;496: 160-168; https://doi.org/10.1016/j.tsf.2005.08.246

[24] Coleman, V.A. and Jagadish, C.,. Basic properties and applications of ZnO, Zinc Oxide Bulk, Thin Films and Nanostructures: Processing, Properties, and Applications, Elsvier Science, 1st Edition,(2006), pp1-20; https://doi.org/10.1016/B978-008044722-3/50001-4

[26] Espitia, P.J.P. Soares, N.D.F.F., dos Reis Coimbra, J.S., de Andrade, N.J., Cruz, R.S. and Medeiros, E.A.A.,. Zinc oxide nanoparticles: synthesis, antimicrobial activity and food packaging applications. Food Biopr.Techn. 2012;5: 1447-1464; https://doi.org/10.1007/s11947-012-0797-6

[27] Reddy, K.R., Karthik, K.V. Prasad, S.B.B., Soni, S.K. Enhanced photocatalytic activity of nanostructured titanium dioxide/polyaniline hybrid photocatalysts, Polyh.2016;120: 169-174; https://doi.org/10.1016/j.poly.2016.08.029

[28] Nosrati R., Olad A., Najjaret, H., Study of the effect of TiO2/polyaniline nanocomposite on the self-cleaning property of polyacrylic latex coating, Surface & Coatings Technology 316 (2017) 199-209; https://doi.org/10.1016/j.surfcoat.2017.03.027

[29] Zhou, B. and Balee, R. Groenendaal, Nanoparticle and Nanostructure Catalysts: Technologies and Markets.Nanotech. Law Busin.,2005;2: 222-228.

[30] Ahmed A. A, Preparation and Characterization of Composites Based onElectrically Conducting Polymer", Ph.D. Thesis, Aligarh Muslim University, 2003.

[31] Ahmed, F., Kumar, S., Arshi, N., Anwar, M.S., Koo, B. H., Lee, C. G., 2011. Defect induced room temperature ferromagnetism in well-aligned ZnO nanorods grown on Si (100) substrate,

Thin Sol. Fil. 2011;51: 98199-8202; https://doi.org/10.1016/j.tsf.2011.03.062

[32] Hussain S. Investigation of structural and Optical properties of Nanocrystalline ZnO, Thesis report, Lincopings University, Sweden, 2006.

[33] F. B and Howe, J. TEM,Transmission Electron Microscopy and Diffractometry of Materials Springer 2007 p, 1-57

[34] Beden,B., Lamy,C., Spectro electro chemistry, Theory and Practice, James Gale(Ed), Plenum Press, New York 1988 p, 220